Archives of Materials Science and Engineering

Volume 37
Issue 2
June 2009
Pages 85-93

International Scientific Journal
published monthly by the
World Academy of Materials
and Manufacturing Engineering

Mechanical strength of Fe/Al structural transition joints subject to thermal loading

L. Tricarico, R. Spina*
Department of Mechanical and Management Engineering (DIMeG), Politecnico di Bari,
Viale Japigia 182, 70126 – Bari, Italy
* Corresponding author: E-mail address: r.spina@poliba.it

Received 22.02.2009; published in revised form 01.06.2009

ABSTRACT

Purpose: The aluminum/steel structural transition joints (STJs) are widely used in shipbuilding industry due to the advantages of joining these two materials with important weight savings while exploiting their best properties. The research objective is the evaluation of mechanical strength of explosion welded structural transition joints by imposing severe thermal loads in specific temperature ranges.

Design/methodology/approach: Mechanical characterization of heat treated specimen have been performed to evaluate the influence of these thermal cycles on final joint resistance and evaluate the product in service. Several specimen aluminum/steel joints have been heated at specific temperature and time and air-cooled in compliance with a Central Composite Design (CCD) experimental plan to investigate the influenced of these factors on inter-metallic layers.

Findings: The micro-hardness measurements have been pointed-out that the hardness of the inter-metallic compounds decreased with the temperature (values greater than 300°C). The processing time influence has been less significant in the observed temporal ranges. This trend has been also confirmed by evaluating the maximum strength of the bond Fe/Al interface. None of the specimens exhibited significant strength variation for thermal loads with temperature lower than 300°C, independently from the processing time.

Research limitations/implications: This methodology is very useful to perform acceptance controls of STJ before use.

Practical implications: These observations are very important to suggest the application of laser techniques to weld this type of joints, thanks to the very narrow localized thermal input.

Originality/value: The paper presents an alternative and cheap way to assess quality of STJs from the mechanical point of view.

Keywords: Metallic alloys; Structural Transition Joint; Heat Treatment; Mechanical properties

Reference to this paper should be given in the following way:

L. Tricarico, R. Spina, Mechanical strength of Fe/Al structural transition joints subject to thermal loading, Archives of Materials Science and Engineering 37/2 (2009) 85-93.

MATERIALS

1. Introduction

Several electronic, naval, aeronautic and automotive components are made by different materials joined together in order to improve mechanical and functional properties. Functionalities provided by clad metals can be grouped into structural, thermal expansion management, thermo-mechanical control, electrical, magnetic, corrosion resistant, joining and cosmetic applications to cite as few [1]. The demand for dissimilar material joints continuously grows because one material can provide only a small spectrum of chemical, physical and mechanical characteristics required for the investigated application respect to the bi- or multi-layer material joints. Moreover considerable weight savings can be achieved by using lightweight materials clad to strength ones

© Copyright by International OCSCO World Press. All rights reserved. 2009

directly [20]. However, the method using the transition joint involves some difficulties in that the transition joint is not easy to produce and is expensive, and the joint is limited in shape [2]. For these reasons, researchers and manufacturers continuously evaluate the application of traditional and/or advanced joining processes to clad dissimilar materials and obtain transition joints optimally. Focusing the attention on steel/aluminum (Fe/Al) joints and shipbuilding industry, the development of lightweight and fast-speed vessels requires a great number of steel/aluminum structural transition joints (STJs) in order to connect aluminum superstructures to the steel hull [3]. Using this solution, the total weight of a ship is reduced due to the lighter aluminum superstructure.

One characteristic feature of all fusion welding processes is the resulting distortion, which is generally unavoidable due to the thermal cycle and the resulting stress and strain fields. Distortion can be compensated by means of a subsequent local heating of the welded structure. Other processes, such as roll bonding process, caused that certain amount of work hardening of materials occurs, and thus the clad sheet must be annealed in order to obtain good properties for the manufacturing processes [4][5] and also avoid corrsosion indesiderable effects [6]. In shipbuilding, for example, buckling of hull and deck structures requires major reworking efforts by flame straightening which can typically be in the order of 15% of the assembly cost of the ship hull [7]. The objective of the present research is the evaluation of the effects of thermal loading on mechanical properties of Fe/Al STJs to assess their functional performances. The tests, based on accepted standards and/or well-known industrial references, employ specimen exposed to several heat loading cycles. These loads reproduce the conditions of the finally assembly of STJs by using fusion welding. This work reports results achieved during experimental activities to evaluate the influence of the thermal loads on final mechanical joint properties in order to suggest feasible operation conditions.

2. Problem position

From the chemical point of view, iron reacts with aluminum forming several Fe_xAl_y inter-metallic compounds. Only small amounts of iron can be dissolved in aluminum and only small amounts of aluminum can be dissolved in iron due to the large difference between the melting points of the two materials. The Al-rich inter-metallic phases are most critical to control respect to the Fe-rich phases to avoid the drastic reduction of joint performances [8]. The complex lattice structures and too high micro-hardness values (up to 800 HV or more) of Al-rich inter-metallic compounds can cause a high interface fragility. These inter-metallic phases occur at temperatures below the melting point of aluminum not only during explosion welding but also when structural transition joints are exposed to thermal loads. The formation rate of the inter-metallic phases is diffusion-driven, thus dependent from time and temperature variables [9][10][11]. Moreover, the effects of the thermal loads directly applied to the STJs must be summed to those generated from fusion welding processes used to assembly the different elements of the product in service. The inter-metallic layer thickness is the main factor to control because components with the inter-metallic layer thickness greater than 10 μm may present very poor mechanical characteristics [12][13].

For this reason, the evaluation of the STJ characteristics at room temperature as well as after the thermal loading is crucial. The mechanical properties of the bond zone are determined by means of tests made in As-clad condition (No preliminary treatment is given to the specimens) and Heat-treated condition (A preliminary heat treatment is directly performed to the specimens) [14]. The specimens are normally heat-treated at 315±14°C (600F±25 °F) for 15 minutes. This temperature-time limit is settled-on by considering that a Fe/Al STJ exposed to a higher time or higher temperature than this limit may present a lower performance life than any as-clad explosion-welded STJs. However, two main considerations have to be made on this temperature-time limit such as: (i) the interaction between the temperature and time variables is not accurately evaluated and (ii) this limit appears to be too conservative for non-conventional welding processes such as laser and electron beam welding, both characterized by very localized low heat input profiles. The main hypothesis to verify is whether a very short time at a high temperature may sufficient to compromise and, in the worst condition, destroy bond properties of explosion-welding STJs, making the application of non-conventional welding process unfeasible. All above considerations shift the manufacturing problem from suppliers to shipbuilders. The interest of an STJ is its direct application instead of the way it is produced.

3. Specimen preparation

A tri-metallic transition joint was chosen for this study due to its industrial importance for the fast vessel construction. The rough material was the Triclad® STJ, a trade name of Merrem & la Porte for steel/aluminum transition joints, produced by with open-air explosion welding. Explosion welding is a solid-state metal-joining process that uses explosive force to create an electron-sharing metallurgical bond between two metal components. Although the explosive detonation generates considerable heat, there is not time for heat transfer to the component metals. Therefore, there is no appreciable temperature increase in the metals [15]. In particular, the selected rough material consisted of an ASTM A516 steel backer plate clad to an AA5083 flyer plate, with commercial purity aluminum (AA1050) interlayer plate placed between the former two. The presence of the AA1050 interlayer was necessary to improve STJ diffusion resistance with both iron and aluminum [16]. The investigated STJ, realized by the supplier in compliance with specification ASTM B898 [1], was analyzed with ultrasonic inspection from the manufacturer to confirm the whole weld interface integrity. STJ specimens of about 28•13•3 mm^3 (Fig. 1) were sectioned by using an abrasive wheel cut-off machine (Discotom-2 of STRUERS) in transverse direction to the length of the rough plate, taking care of minimizing the mechanical and thermal distortions of the Fe/Al interface. The specimen surfaces were smoothly ground to give a uniform finish and cleaned before putting them in the heat treatment oven.

Each specimen was heated at specific temperature and time in compliance with the Central Composite Design (CCD) experimental plan and cooled outside the oven to the room temperature. The temperature of the heat treatment oven was rapidly reached by applying a high heat power and then maintaining this temperature for time sufficient to guarantee stationary conditions. The specimen was then inserted into the oven. This process was repeated for all specimens. The CCD design is a factorial or fractional factorial design (with center points) in which "star" points are added to estimate curvature [17]. The main CCD factors were the temperature and time, ranging between 100 and 500°C and 5 and 25 minutes, respectively. The CCD center point,

replicated five times, was fixed at 300°C for 15 minutes, according to the limit of the heat treated condition. The entire plan, shown in Table 1, also included the as-clad condition (ID 12) and near-fusion condition (ID 13).

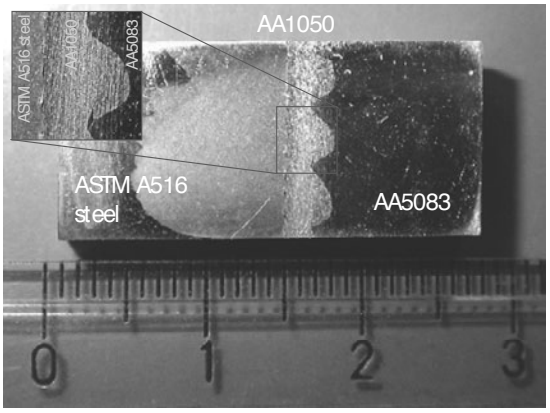

Fig. 1. Triclad® STJ

Table 1.
Central Composite DOE

Specimen ID	Temperature (°C)	Time (minutes)
1	100	5
2	100	25
3	500	5
4	500	25
5-6-7-8-9	300	15
10	300	1
11	300	29
12	18	15
13	582	15

4. Micro-hardness evalution

Micro-hardness test were performed to measure the strength of Fe/Al interface in a non-destructive way as well as its variation under heat thermal loads. The specimens were prepared by grinding with 200 to 1000-grit silicon carbide papers, followed by mechanical polishing from 6-µm to 1-µm diamond abrasive on short nap clothes. Etching was then performed on the steel side of specimens with Nital solution (2 mL HNO_3 and 98 mL of C_2H_5OH) in distilled water for 15 seconds in order to highlight grain structures as well as inter-metallic phases. Keller's reagent (5 mL HNO_3 and 190 mL of H_2O) was applied for 15 seconds to aluminum side to point macro-structures. A Vickers micro-tester (HX-1000TM of REMET) mounting a 40x objective and 15x eyepieces lenses was used, setting the indentation load to 200 g for 15 s, in compliance with ASTM standard E92. Analysis points were sufficiently spaced to eliminate the effect of neighboring indentations while evaluating existing materials and phases. Five indentations were taken at specific locations at and far from Fe/Al interface (Fig. 2.) for three times and results then averaged. The area of measure was randomly selected for each specimen by respecting the condition that at least one ripple was contained in it. The hardness result was the average value of all inter-metallic phases embraced by the indenter diagonal. The results reported in Table 2 pointed-out that hardness values of AA5083, AA1050 and ASTM A516 steel (Point A, B, D and E) were slightly affected from heat treatments. The justification of this behavior could be that longer time at investigated temperatures should be necessary to allow greater diffusion fluxes. The hardness of the inter-metallic compounds (point C) was greatly influenced by temperature and time factors. The analysis of variance (ANOVA) of the inter-metallic hardness response variable related to point C pointed-out that increases in time and temperature lowering hardness (Fig. 3). In particular, temperature square, followed in order of importance from temperature and time square, were the main significant terms of the quadratic model (Table 3). This model presented R^2 and adjusted R^2 values equal to 88% and 79%. The reduction in hardness could be caused by the inter-metallic transformation from hard to soft phases.

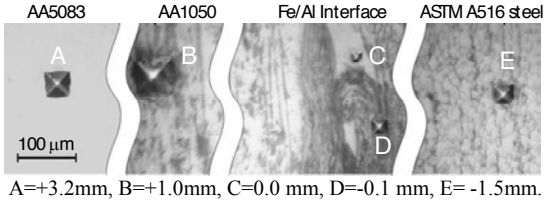

A=+3.2mm, B=+1.0mm, C=0.0 mm, D=-0.1 mm, E= -1.5mm.

Fig. 2. Vickers indentations

Table 2.
Vickers results

Specimen			Indentation ID (HV)				
ID	T (°C)	t (min)	A	B	C	D	E
1	100	5	105	46	583	266	195
2	100	25	107	41	534	245	178
3	500	5	81	31	430	242	182
4	500	25	83	28	483	239	166
5	300	15	91	44	554	235	186
6	300	15	81	45	593	238	180
7	300	15	97	44	618	247	183
8	300	15	89	42	582	278	175
9	300	15	81	39	582	294	183
10	300	1	107	43	543	246	186
11	300	29	85	40	527	245	174
12	18	15	100	41	545	246	179
13	583	15	72	30	476	192	158
Mean			91	40	542	247	179
Std Dev.			12	6	53	24	9

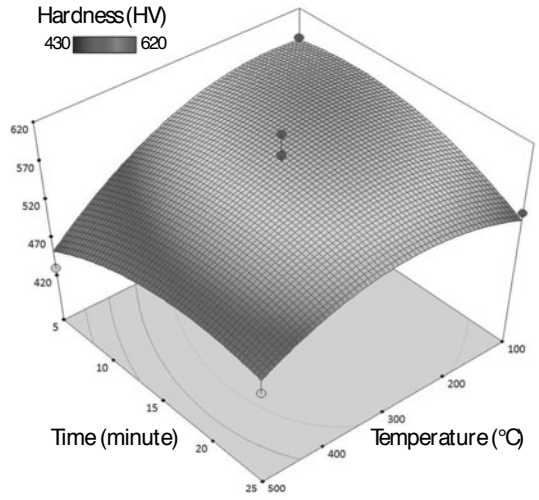

Fig. 3. Response surface of inter-metallic hardness

Table 3.
ANOVA – Vickers Results of Point C

Model	27854.04	5	5570.81	11.75	0.0027
Temperature	8916.54	1	8916.54	18.81	0.0034
Time	34.79	1	34.79	0.073	0.7942
Temperature·Time	4726.56	1	4726.56	9.97	0.0160
Temperature^2	10780.71	1	10780.71	22.75	0.0020
Time^2	5084.84	1	5084.84	10.73	0.0136
Residual	3317.41	7	473.92		
Total	31171.45	12			

Equation of the response surface

HV = +560.674 +1.658E-01·Temperature +3.165·Time +1.719E-02·Temperature·Time -9.84169E4·Temperature^2 -0.2704E-01·Time^2

5. SEM observations

The observations of the superficial morphology of heat-treated specimens and related micro-analysis were performed with the thermionic SEM Philips XL 40 (Fig. 4.), located at ENEA.

The strong beam of electrons of this SEM machine, called primary electron beam, is produced by the thermionic emission of the Lanthanum Hexaboride (LaB_6) filament, preferred to tungsten filament because of its long life and reasonable stability of electron beam emission. The primary beam of electrons thus emitted by thermionic emission interacts with the top atomic layers of surface of the sample. This gives out a variety of signals that can be collected and processed to derive a good quality of information about the morphology of the sample, atomic contrast in the sample and the elemental composition of the top surface of the material. The microscope is equipped with a three-axes motorized stage (X,Y and rotation) and operates within a Microsoft Windows environment. Automated focusing, astigmatism correction and contrast/brightness as well as rotation-free focusing, power zoom, split screen, on screen X and Y measurements, graphics editor and image manipulation facilitate the operation. Beside the standard scintillator detector, a solid state backscattered detector is mounted. A CCD camera allows the user to monitor the inside of the specimen chamber. The STJ specimens for SEM analyses were prepared by grinding with 200 to 1000-grit silicon carbide papers, followed by mechanical polishing from 6-μm to 1-μm diamond abrasive on short nap clothes. In this case, the achievement of a mean surface roughness less than 1-μm was crucial to obtain high quality image.

Fig. 4. SEM at Philips XL 40 ENEA - Dept. FIM

The SEM analyses were mainly performed from the qualitative point of view by visually inspecting morphology of the Fe/Al interface. The back-scattered electron (BSE) images near the specimen Fe/Al interface showed the AA1050 in dark grey, the ASTM A516 steel in the light grey the "wavy" interfacial area with different gray, in function existing Fe_xAl_y intermetallics.

Fig. 5 is one of the acquired BSE images for the as-clad specimen. Fig. 6. reports the magnification of the rectangular circumscribed area shown in Fig. 5, in order to point out several aspects. The thin layer between steel and aluminum consisting of different type of intermetallics. The dark grey ones were rich of the aluminum phase exists while the light gray ones are rich of the iron phase. In addition, ripples are made of iron-rich intermetallics. In fact Fig. 7 reports the results of the micro-analysis of the area indicated from the arrow.

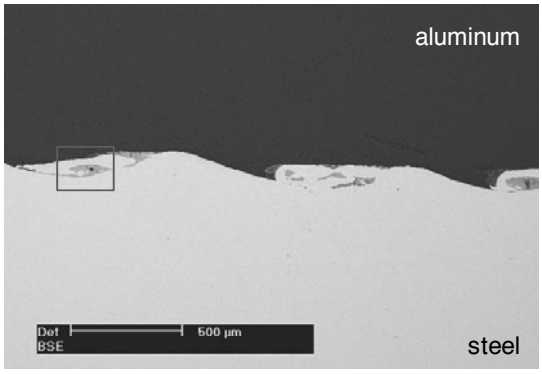

Fig. 5. As-clad specimen

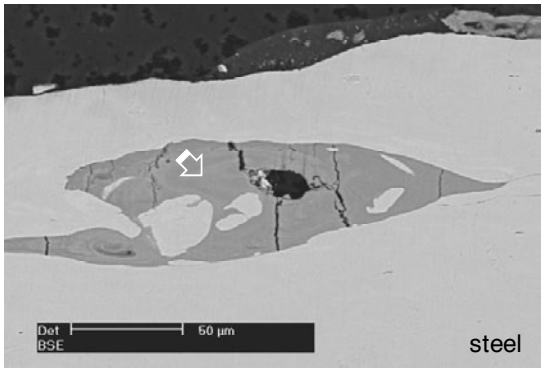

Fig. 6. Details of as-clad specimen

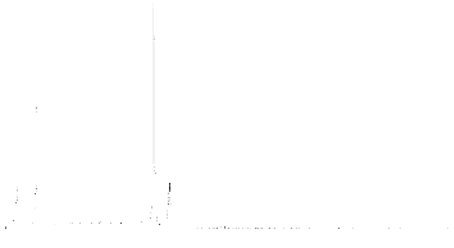

Fig. 7. Quantitative analysis

As figure shows, the Fe counter was greater than the Al counter. With energy dispersive x-ray spectrometers (EDS), chemical compositions was determined quickly. Despite the ease in acquiring x-ray spectra and chemical compositions, the potentially major sources of error were minimized by optimizing the operative conditions necessary to improve the statistical meaning of the electron counter. In particular, the scanning area was equal to 1 μm^2, the incident energy was 25 keV on the specimen surface with a working distance of 10 mm (in this way the x-ray take-off distance was equal to 35°), the electronic current was tuned in order to generate a X-ray counter rate of 2000 pulse per second and the effective counter time was equal to 100 s [18].

A different situation was identified by analyzing the heat-treated specimen at 500°C for 15 minutes. The diffusion zone at the interface is shown in a grey contrast and its width is increased with temperature. The BSE image clearly indicate that the diffusion zone consists of several layers (arrow I and arrow II) in the Fe/Al interface (Fig. 8). This particular feature cannot be resolved by using an optical microscope. Enhancement in heating temperature results in important changes in the interface microstructure. Two distinct reaction layers formed between the aluminum and steel at the interface. These results pointed out the importance of the time variable on inter-metallic thickening. In fact, the average Fe_xAl_y layer thickness increased with temperature and time, creating more classes of intermetallics compounds because of diffusion.

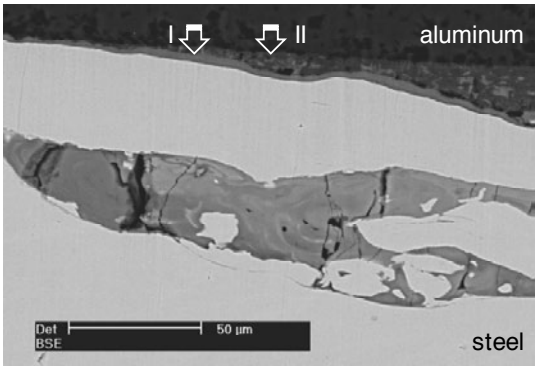

Fig. 8. Details of heat treated specimen

6. Ram Tensile Test

The strength of the welding zone is evaluated by Ram Tensile Test. During the test, the force is applied to the direction perpendicular to the planes delimiting different material interface. A specimen with a particular parallelepiped/cylindrical shape is used in order to concentrate stresses in the section just above the transition area that corresponds to the bond interface, as Fig. 9 shows. The MIL-J-24445A standard, specifies maximum dimensions of the bi-material specimen but its principles can be easily extended to tri-material joints. In this last case, the strength of the steel/AA1050 bond interface is estimated rather than that of the AA5083/AA1050 one.

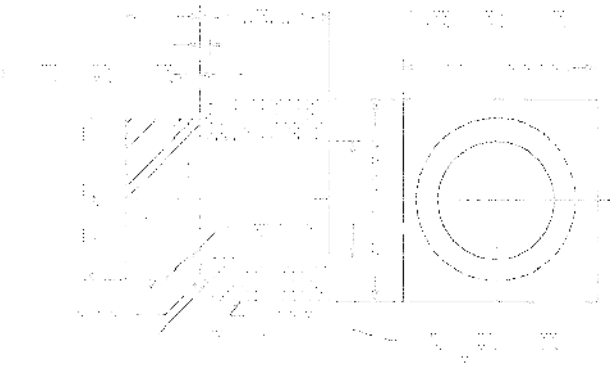

Fig. 9. Specimen

The specimen, punch and matrix prescribed by the above cited standard are reported in Fig. 10.The matrix is fixed while the punch moves in contact with the bond interface, compressing it until rupture. The MIL-J-24445A standard does not give values or suggestions linked to testing parameters (e.g. punch speed) and/or specimen clamping. The specimen is simply rested on the matrix top surface, allowing its rotation around the cylindrical axis. In the hypothesis that the pressure between punch and specimen during contact is uniform, the applied load can be considered as axial-symmetric. The thickness D of the bond zone is always equal to 1.72±0.1 mm, independently from the values of steel and aluminum thicknesses. The thickness D is achieved by simply varying the hole depth.

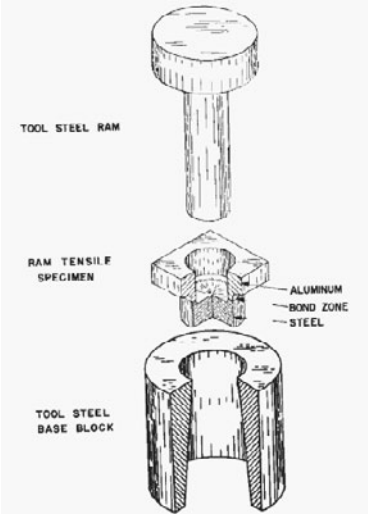

Fig. 10 Testing equipment

The testing equipment, designed and realized in compliance with the MIL-J-24445A standard, allowed the easy set-up on an universal tensile testing machine. The equipment consisted of a screwed punch and a two elements matrix with a changeable cylindrical insert (Fig. 11).

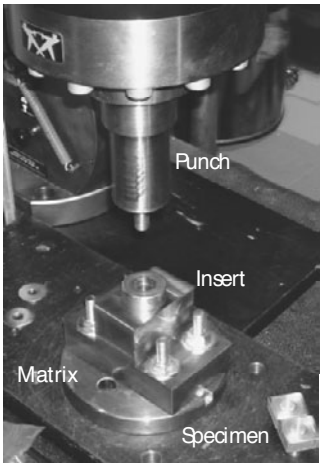

Fig. 11. Testing equipment in the laboratory

The punch is mounted on the top mobile crosshead of the INSTRON 4485 machine while the matrix is fixed to the machine basement with bolts and nuts. The choice of the changeable insert was justified by the need to substitute the insert in case of high wear conditions as well as to select the proper tolerance gap with the specimen. The correct alignment between the punch and specimen axes to avoid bending effects was realized by means of a guided groove in the low part of the matrix. The pressure of the punch caused tensile loads on specimen bond interface. The maximum tensile stress value recorded during test was used to assess the joint strength for several temperature-time cycles. The minimum value of the tensile stress to consider the joint as good should be greater than 75 N/mm^2. The designed experimental plan for mechanical testing was extended respect to the plan used for micro-hardness evaluation in order to preserve continuity with previous investigation, evaluate more critical conditions associated to higher time and/or temperatures and improve knowledge about mechanical strength limits of tri-material transitions joints. Metallographic examinations revealed that the heat-treated joints properties remained quite equal to those of as-clad specimen for temperatures lower than 300°C and processing times lower than 15 minutes. The new experimental plan is reported in

Fig. 12, in terms of temperature-time couples, while results are reported in Table 4. For each test, the force-displacement data was acquired in real-time. The punch speed was set to 0.05 mm/s for all tests.

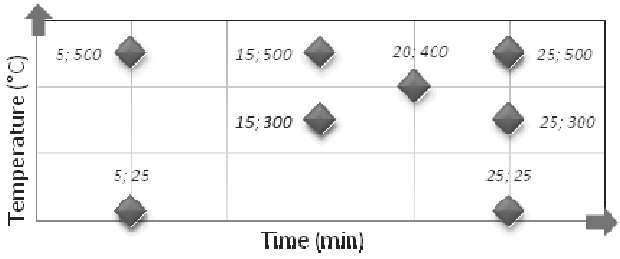

Fig. 12. New experimental plan

Table 4.
Ram tensile test results

Specimen ID	Temperature (°C)	Time (minutes)	Force (kN)	Strength (MPa)
HTRT1	25	5	29.4	233.7
HTRT2	300	15	30.1	239.3
HTRT3	500	25	4.3	34.2
HTRT4	300	25	25.2	200.3
HTRT5	400	20	16.4	130.4
HTRT6	500	15	4.8	38.2
HTRT7	500	5	17.8	141.5
HTRT8	25	25	29.9	237.7

Some important considerations can be carried-out by analyzing results of Table 4.The maximum strength of the as-clad specimen as well as specimens processed at 300 °C were greater than minimum value of 120 MPa certified by the material supplier. In addition, the specimen resistance was mainly supported by the small thickness of AA1050, considering that the maximum strength of this commercial alloy was about 180-190 MPa at high cold work conditions. These values suggested that the thermal cycles may reduced the cold work conditions, with consequent reduction of the maximum strength of the tri-material joint. The specimen behavior changed when processing temperature was greater than 300°C. Based on the above results,

temperature was the main factor causing the lowering of the specimen mechanical strength. The same considerations arose from the analysis of the load-displacement data. HTRT1 and HTRT2 specimens were characterized by the same curves, with equivalent values of the maximum load (L) and displacement (D), as Fig. 13 reports.

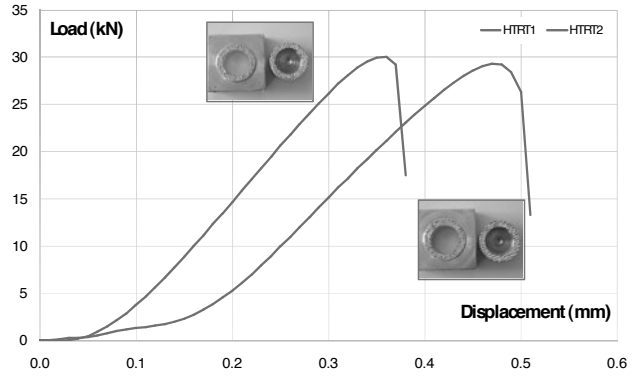

Fig. 13. L/D curves of HTRT1 and HTRT2 specimens

This behavior pointed-out that mechanical properties were not greatly altered from processing temperature and time, even if *HTRT2* specimen stayed in the oven at 300°C and *HTRT1* specimen was thermally untreated. The maximum supported load started to drop when specimen were treated at temperatures higher than 300°C. The *HTRT5* specimen, processed at 400°C for 20 minutes, and *HTRT7* specimen, processed at 500°C for 5 minutes, were accomplished by the reduction of the maximum load value with the increase of the maximum displacement (Fig. 14). In fact, the load-displacement curves of the two specimens were perfectly equivalent from the mechanical point of view. The maximum load drastically drop for higher temperatures, as *HTRT3* specimen, processed at 500°C for 25 minutes, witnessed. The reduction of the mechanical strength with temperature and time becomes more evident by the ANOVA reported in Table 5, with results in graphical form are reported in (Fig. 15)

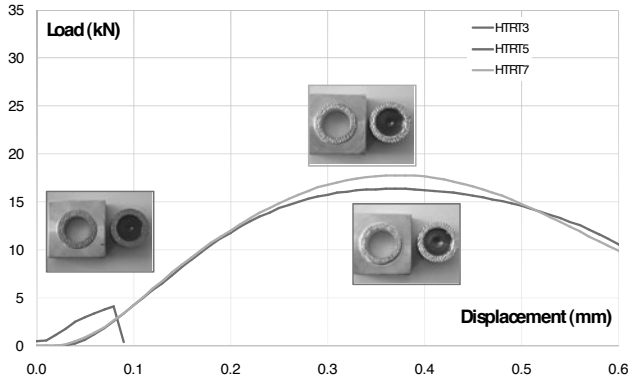

Fig. 14. L/D curves of HTRT3, HTRT5 and HTRT7 specimens

Table 5.
ANOVA – Mechanical strength

Model	50191.04	5	10038.21	20.21	0.0478
Temperature	26285.52	1	26285.52	52.91	0.0184
Time	3962.75	1	3962.75	7.98	0.1058
Temperature·Time	3391.77	1	3391.77	6.83	0.1205
Temperature^2	12417.82	1	12417.82	25.00	0.0378
Time^2	951.94	1	951.94	1.92	0.3005
Residual	993.55	2	496.77		
Total	51184.59	7			

Equation of the response surface

Strength = + 253.6562 +0.83888·Temperature -8.35064·Time -0.01218·Temperature·Time -1.876E -03·Temperature^2 +0.28422·Time^2

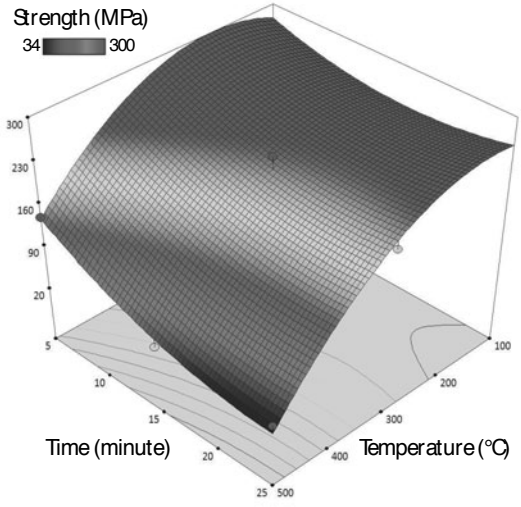

Fig. 15. Mechanical strength

The justification of this fragile behavior was that the heat treatment at high temperature promoted the inter-metallic redistribution at Fe/Al bond interface, with consequence growth of the inter-metallic thickness, causing the lowering of the mechanical properties. This hypothesis has been confirmed by previous works [19] in which the influence of the thermal loading of the Fe/Al explosion welded joints was investigated by measuring the extension and thickness of inter-metallic compounds at Fe/Al interface. The metallographic analysis measurements have pointed-out that the band extension was mainly influenced by the temperature because the increase of the band extension with increasing temperature has been recorded. Observing the evolution of the inter-metallic band thickness, it has been observed that thickness at 500°C after 5 minutes was half than that obtained after 25 minutes.

Another important aspect took into account was the shape of the fractured surfaces of the thermally loaded specimens. The fracture surfaces were characterized by a ductile fracture with

very low appreciable deformation and/or absent signs of gross plastic deformation. This fracture may be justified by the presence of a continuous diffuse inter-metallic layer that triggered micro-cracks. The Fig. 16 reports the fractures aspects of *HTRT1*, *HTRT2* and *HTRT3* specimens.

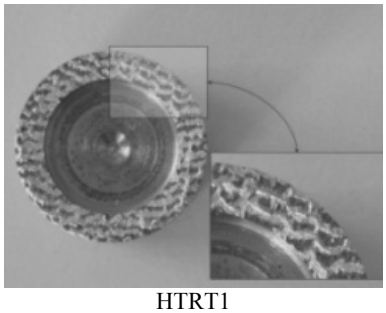

HTRT1

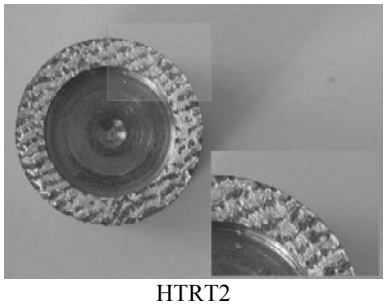

HTRT2

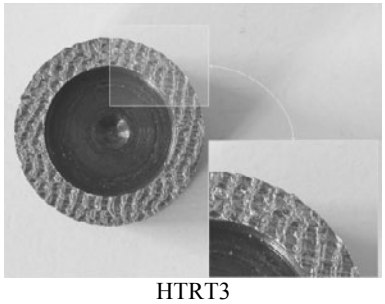

HTRT3

Fig. 16. Surface fractures

The pattern of the *HTRT1* specimen is very irregular with evident differences between peaks and voids. These difference between peaks and voids were lower in case of *HTRT3* specimen, as the fragile fracture of the specimen at the end of the test shows. The surface aspect of the *HTRT2* specimen seemed to be intermediate between the other two specimen surfaces, corroborating results achieved during the ram tensile test in terms of maximum load and displacement.

7. Conclusions

In this work the influence of different thermal loads on mechanical strength of the Fe/Al explosion welded joints has been investigated. The micro-hardness measurements have pointed-out that the hardness of the inter-metallic compounds decreased with the temperature (values greater than 300°C). The processing time influence has been less significant in the observed temporal ranges. The effect of time and temperature has been analyzed in term of hardness variation in the STJ. The biggest variation has been registered in the inter-metallic zone and, referring to the as-clad specimen, the hardness decreased with both temperature and time. This trend has been also confirmed by evaluating the maximum strength of the bond Fe/Al interface. None of the specimens exhibited significant strength variation for thermal loads with temperature lower than 300°C, independently from the processing time. The mechanical strength rapidly drop after this critical temperature value. Specimens subjected to thermal loads for temperature near the melt temperature of aluminum alloys were characterized by very low values of stress and deformation, compared to the values of untreated specimens.

Acknowledgements

The authors wish to thank Dr. Marco BRANDIZZI of the Fiat Research Center (CRF), Dr. Donato SORGENTE of DIMEG-Politecnico di Bari, Dr. Marco VITTORI ANTISARI of ENEA – Casaccia Research Center and Laura CAPODIECI of ENEA – Dept. FIM - Composites & Nanostructured materials Section for their precious collaborations.

Additional Information

The present research is only a part of activities performed by Consortium for Laser and Electron Beam Applications (CALEF), the main members of which are the CRF, ENEA, Polytechnic of Bari and Rodriquez Cantieri Navali SPA. In particular, Rodriquez Cantieri Navali SPA directly funded this research through the ENVIROALISWATH project.

References

[1] L. Chen, Z. Yang, B. Jha, G. Xia, J.W. Stevenson, Clad metals, roll bonding and their applications for SOFC interconnects, Journal of Power Sources 152 (2005) 40-45.

[2] T. Watanabe, H. Takayama, A. Yanagisawa, Joining of aluminum alloy to steel by friction stir welding, Journal of Materials Processing Technology 178 (2006) 342-349.

[3] R.M. Chao, J.M. Yang, S.R. Lay, Interfacial toughness for the shipboard aluminum/steel structural transition joint, Marine Structures 10 (1997) 353-362.

[4] D. Kuc, G. Niewielski, I. Bednarczyk, The influence of thermomechanical treatment on structure of FeAl intermetallic phase-based alloys, Journal of Achievements in Materials and Manufacturing Engineering 29/2 (2008) 123-130.

[5] J.E. Lee, D.H. Bae, W.S. Chung, K.H. Kim, J.H. Lee, Y.R. Cho, Effects of annealing on the mechanical and interface properties of stainless steel/aluminum/copper clad-metal sheets, Journal of Materials Processing Technology 187-188 (2007) 546-549.

[6] J. Cebulski, S. Lalik, R. Michalik, Corrosion resistance of FeAl intermetallic phase based alloy in water solution of NaCl, Journal of Achievements in Materials and Manufacturing Engineering 27/1 (2008) 15-18.
[7] F. Vollertsen, Developments and trends in laser welding of sheet metal, Advanced Materials Research 6/8 (2005) 59-70.
[8] G. Sierra, P. Peyre, F. Deschaux-Beaume, D. Stuart, G. Fras, Steel to aluminium key-hole laser welding, Materials Science and Engineering A 447 (2007) 197-208.
[9] D. Naoi, M. Kajihara, Growth behavior of Fe_2Al_5 during reactive diffusion between Fe and Al at solid-state temperatures, Materials Science and Engineering A 459 (2007) 375-382.
[10] S. Kobayashi, T. Yakou, Control of intermetallic compound layers at interface between steel and aluminum by diffusion-treatment, Materials Science and Engineering A 338 (2002) 44-53.
[11] V. Jindal, V.C. Srivastava, Growth of intermetallic layer at roll bonded IF-steel/aluminum interface, Journal of Materials Processing Technology 195 (2008) 88-93.
[12] Rattana Borrisutthekul, Taisei Yachi, Yukio Miyashita, Yoshiharu Mutoh, Suppression of intermetallic reaction layer formation by controlling heat flow in dissimilar joining of steel and aluminum alloy, Materials Science and Engineering A 467 (2007) 108-113.
[13] P. Peyre, G. Sierra, F. Deschaux-Beaume, D. Stuart, G. Fras, Generation of aluminium–steel joints with laser-induced reactive wetting, Materials Science and Engineering A 444 (2007) 327-338.
[14] American Bureau of Shipping, Materials and Welding 2000, Supplementary Requirements for Naval Vessels, Part 2 Chapter 11, Section 6, Aluminum/Steel Bimetallic Transition Joints.
[15] ASM Handbook Volume 6: Welding, Brazing, and Soldering, Fundamentals of explosion welding, http://products.asminternational.org/hbk/index.jsp
[16] J. Bankers, A. Nobili, Aluminum-Steel Electric Transition Joints - Effects of Temperature and Time upon Mechanical Properties, Proceedings of the 131st Annual Meeting & Exhibition of The Minerals, Metals & Materials Society, (TMS), Seattle, USA, 2002.
[17] D.C. Montgomery, Design and Analysis of Experiments , 5th Ed., J.Wiley and Sons 1, 2000.
[18] L. Capodiceci, Analyss of Explosion welding steel /aluminum transition joint with Scanning Electronic Microscope and X-Ray Microanalysis, ENEA Internal Technical Report n. RT/ENEA/ 06/11 of FIM COMP Dept.
[19] L. Tricarico et al., Effects of laser welding on properties of Fe/Al explosion welded structural transition joints, ATA Proceedings of the 2nd International Conference on "Advanced Materials and Technologies for Transportation Industry", ELASIS, Pomigliano D'Arco, Italy, 2007.
[20] K. Mroczka, J. Dutkiewicz, L. Lityńska-Dobrzyńska, A. Pietras, Microstructure and properties of FSW joints of 2017A/6013 aluminium alloys sheets, Archives of Materials Science and Engineering 33/2 (2008) 93-96.